

Using *JMatPro* to Model Materials Properties and Behavior

N. Saunders, Z. Guo, X. Li, A.P. Miodownik, and J.-Ph. Schillé

This article describes the development of a new multi-platform software program called JMatPro for calculating the properties and behavior of multi-component alloys. These properties are wide ranging, including thermo-physical and physical properties (from room temperature to the liquid state), time-temperature-transformation/continuous-cooling transformation diagrams, stress/strain diagrams, proof and tensile stress, hardness, coarsening of γ' and γ'' , and creep. A feature of the new program is that the calculations are based on sound physical principles rather than purely statistical methods. Thus, many of the shortcomings of methods such as regression analysis can be overcome. With this program, sensitivity to microstructure can be included for many of the properties and the true inter-relationship between properties can be developed, for example in the modeling of creep and precipitation hardening.

INTRODUCTION

Tools that utilize thermodynamic modeling to explore the equilibrium and phase relationships in complex materials are being used increasingly in industrial practice.¹ These tools provide significant benefit, but they often fail to directly provide the information required. For example, thermodynamic modeling helps toward the understanding of changes in phase constitution of a material as a function of composition or temperature. However, there is then a gap in translating this information into the properties targeted by the end user, (e.g., time-temperature-transformation [TTT] diagrams, mechanical properties, and thermo-physical and physical properties.

The jump from thermodynamic

calculation to the final understanding of materials properties is significant. It can usually only be achieved through further experimentation if quantitative information is required or through the knowledge and experience of the user if guidance of a more qualitative nature suffices. To overcome these limitations, a new computer program has been developed² called *JMatPro*, an acronym for Java-based materials properties. The program was developed to augment the thermodynamic calculation by incorporating various theoretical materials models and properties databases that allow a quantitative calculation for the requisite materials property to be made within a larger software structure.

THERMODYNAMIC CALCULATIONS

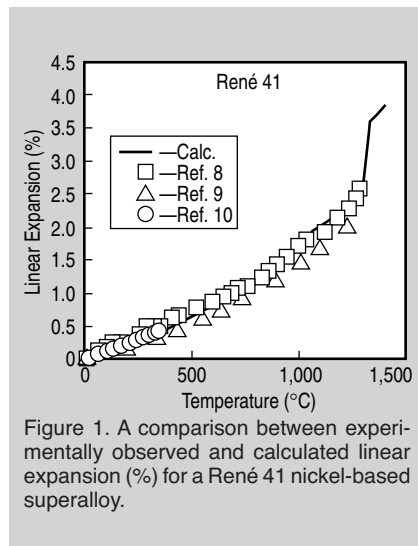
The current software utilizes core minimization routines developed for the *PMLFKT* software program by Lukas et al.³ and recently extended by Kattner et al.⁴ to multicomponent alloys. These subroutines have been converted from Fortran to C and, in addition, a

comprehensive set of new subroutines written in C/C++. These new subroutines provide a variety of benefits, including facilities for setting automatic start points; original algorithms to ensure that highly reliable results for multi-component, multiphase equilibria can be routinely calculated; algorithms for stability checking that also continually monitor the composition of the various phases that may have miscibility gaps or the potential for ordering; and highly robust routines for finding phase boundaries.

THERMO-PHYSICAL AND PHYSICAL PROPERTIES

In the Solid State

Because thermo-physical and physical properties are critical input for software programs dealing with process modeling, the *JMatPro* project has developed an extensive database for the calculation of physical properties that can be linked to its thermodynamic calculation capability. For individual phases in multicomponent systems, properties such as molar volume, thermal conductivity, Young's modulus, and Poisson's ratio are calculated using simple pair-wise mixture models. These models are similar to those used to model thermodynamic excess functions in multicomponent alloys.¹ Once the property of the individual phase is defined, the property of the final alloy can be calculated using mixture models that can account for the effect of microstructure on the final property.^{5,6} Such models, which were developed for two-phase systems, have been extended to allow calculations to be made for multiphase structures.⁷ However, when the properties of the phases are similar, most types of phase-mixture models



tend toward the linear rule of mixtures. The power of the models becomes apparent when phases with very different properties exist in the alloy, for instance, in the case of modulus calculations when high levels of carbides or borides are present in relatively soft metallic matrices (e.g., SiC in an aluminum solid solution).

Extensive databases of relevant parameters exist for most of the major phases in Al, Fe, Mg, Ni, and Ti alloys and have been tested extensively in the solid state against experimental measurement. Figure 1 shows a comparison between calculated and experimentally reported⁸⁻¹⁰ linear expansion for a René 41 nickel-based superalloy.

Utilizing well-established relationships between certain properties (e.g., thermal and electrical conductivity) allows other properties to be calculated without using further databases, so that the following properties can be modeled: volume, density, expansion coefficient, Young's, bulk and shear moduli, Poisson's ratio, thermal conductivity and diffusivity, electrical conductivity, and resistivity. Furthermore, it is possible to

calculate lattice parameters for the γ and γ' phases in nickel-based superalloys and calculate γ/γ' mismatch as a function of temperature.

During Solidification

The thermo-physical and physical properties of the liquid and solid phases are critical components in casting simulations. Such properties include the fraction solid transformed, enthalpy release, thermal conductivity, volume, and density, all as a function of temperature. However, due to the difficulty in experimentally determining such properties at solidification temperatures, little information exists for multicomponent alloys. The calculation of physical properties has, therefore, been extended to include their calculation for solidification.

Recently, the application of so-called Scheil-Gulliver (SG) modeling via thermodynamic modeling has led to the ability to predict a number of critical thermophysical properties for alloys such as nickel-based superalloys,¹¹⁻¹³ aluminum alloys,^{14,15} and cast irons.¹⁶ Such calculations can be computationally

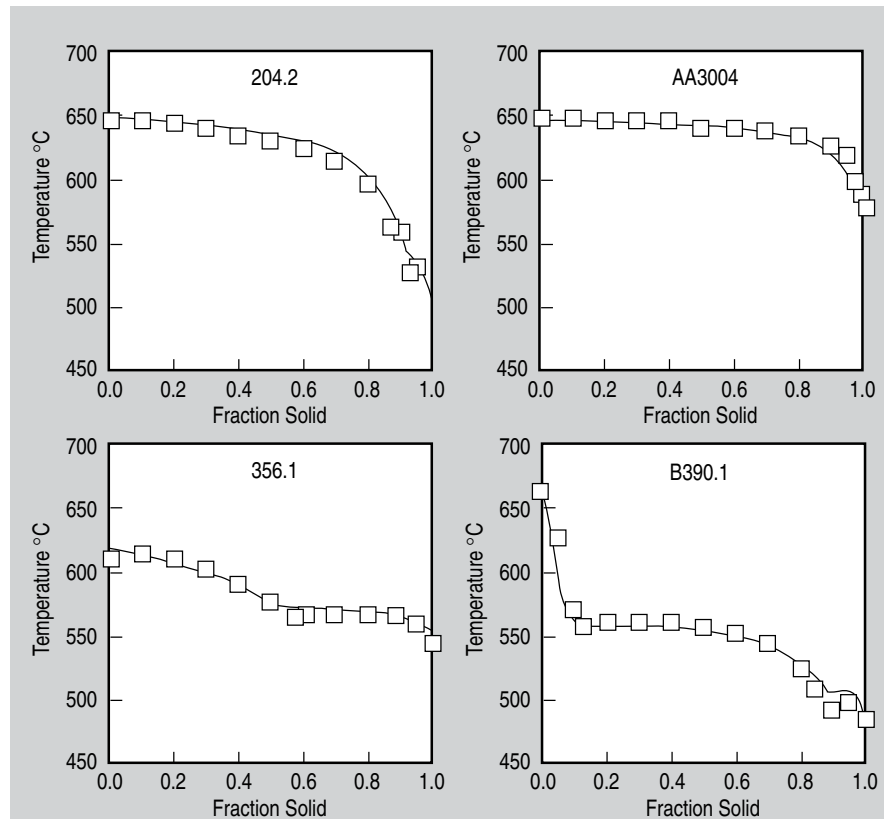


Figure 2. The fraction solid vs. temperature plots for various aluminum alloys calculated under Scheil-Gulliver conditions with experimental results (\square) of Backerud et al. shown for comparison.

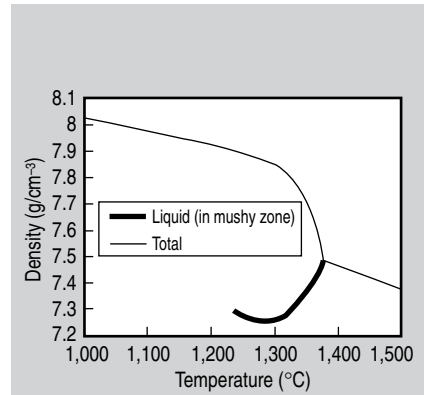


Figure 3. The calculated density of a SRR99 single-crystal superalloy during solidification. The bold line shows the density of the liquid in the mushy zone.

ally fast and readily used within solidification packages such as *ProCAST*.¹¹ The model assumes that solute diffusion in the solid phase is small enough to be considered negligible and that diffusion in the liquid is fast enough to assume that diffusion is complete. Such a process is quite simple to model using thermodynamic calculations based on the CALPHAD method and has been described in numerous publications.^{1,11,17,18} Some back diffusion will occur, but in many cases the SG assumption leads to good results for much of the solidification range and can be used to obtain high-quality input for casting simulations.¹⁷

For the case of steels, carbon and nitrogen diffuse rapidly in the solid state and it is possible to consider that complete back diffusion of these elements will occur. Such a model has been implemented in *JMatPro* by considering that carbon and nitrogen will diffuse sufficiently rapidly such that their composition in the growing austenite or ferrite phases will be equal to that of the solid at the growing solid/liquid interface.¹⁹

Aluminum alloys provide an excellent example of the success of the SG model. Backerud et al.²⁰ experimentally determined the fraction solid vs. temperature behavior of 40 aluminum alloys and obtained detailed information on the phases formed during solidification. All of these alloys have been modeled and the predicted results for both fraction solid vs. temperature and phase formation compared with experiment. Figure 2 shows typical

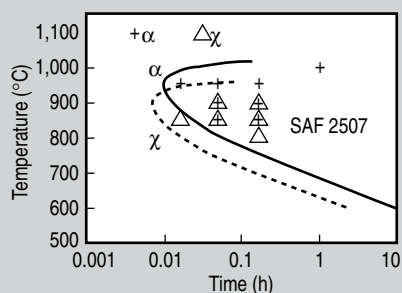


Figure 4. The calculated TTT diagram for a SAF 2507 duplex stainless steel with experimentally observed²⁸ TCP phases shown for comparison.

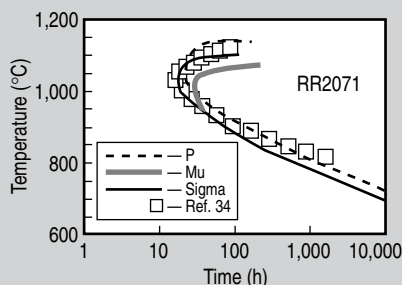


Figure 5. A comparison between a calculated and experimentally observed²⁹ TTT diagram for a RR2071 single-crystal nickel-based superalloy.

results that are obtained.

The physical properties of the liquid phase in Al-, Fe-, Mg-, Ni-, and Ti-based alloys have also been modeled^{19–24} and can be combined with SG-based calculations and physical properties for the solid state to provide soundly based changes in physical properties during the casting process. Figure 3 shows the calculated density of a SRR99 single-crystal alloy during solidification. Fine detail can be obtained, such as the density of the liquid in the mushy zone (Figure 3), which can be utilized to calculate casting defects. A significant advantage of the current model is that properties such as elastic moduli can be used for the modeling of residual stress in castings.

TTT AND CCT DIAGRAMS

As part of the goal of extending the calculation of equilibrium phase stability to include kinetics, work has been undertaken to extend *JMatPro*'s capability to TTT and continuous-cooling transformation (CCT) diagrams. This has been achieved by using the Johnson-Mehl-Avrami equation²⁵ as

a basis. The original equation is for spherical particles, and work has been done^{2,26} to include the effect of non-spherical precipitates by incorporation of the effect of shape in the basic equations after Martin et al.²⁷ Work is ongoing to build up the requisite diffusion databases, assess the typical nucleation and shape characteristics for the various types of precipitate, and validate the approach by comparison with experiment.

An advantage of the current modeling method is that few input parameters need to be empirically evaluated. Where empirical values are used, for example, in consideration of shape and nucleant density, specific values have been defined for the various precipitates (i.e., σ , χ , μ , α -Ti) in each material type. Once these values are defined, they have then been self-consistently applied and the model can therefore be used in a predictive fashion.

Figure 4 shows the comparison between experimentally observed²⁸ and calculated²⁶ transformation behavior in a SAF2507 austenitic stainless steel. The curves are calculated for 0.5% transformation of σ and χ . There is good overall agreement with observed behavior, which is typical of the accuracy that can be obtained. Figure 5 shows a comparison between the experimentally observed TTT diagram for a single-crystal alloy RR2071²⁹ and calculation. For this case, the number of potential nucleation sites has been taken as being considerably lower than that for a normal superalloy where the formation of TCP phases often occurs at grain boundary sites, which are absent in the single-crystal alloy. It is also notable that the stability of the σ , μ , and P phases is very similar, an observed feature of rhenium-containing single-crystal alloys.^{29,30}

The present approach has been extended to the transformation kinetics in γ' and γ'' hardened nickel-base superalloys² (e.g., 718 alloy³¹) and titanium alloys. In the latter case, the low-temperature phase α precipitates out from the high-temperature β . Two types of α precipitate are considered, those at the prior β grain boundaries (GB) and those in the prior β grain interior (bulk) that have a higher barrier to nucleation. Nucleant densities

consistent with formation at GBs and dislocation sites³² have been utilized. Figure 6 shows such a calculated diagram for a Ti-1023 alloy with experimentally observed points^{33,34} superimposed.

It is possible to convert TTT diagrams to continuous-cooling-transformation diagrams using well-known additivity rules.³⁵ A calculated CCT diagram for Ti-1023 is shown in Figure 7. It is also possible using CCT calculations to calculate Jominy Hardenability in high-strength low-alloy steels^{36,37} and this capability has been incorporated in *JMatPro*.

COARSENING OF γ' PARTICLES IN NI-BASED SUPERALLOYS

An important feature of nickel-based superalloys is coarsening of γ' at high temperatures, both for processing and service life. Recently, Li et al.³⁸ have shown how a combination of CALPHAD calculations and the existing theory of Ostwald ripening^{39–41} can be used to calculate coarsening rates of nickel-based superalloys to a high level of accuracy. The CALPHAD

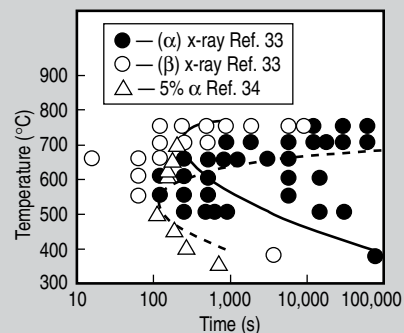


Figure 6. An experimentally observed^{33,34} and calculated TTT diagram for Ti-1023. Full lines indicate α (GB), dashed lines denote α (bulk).

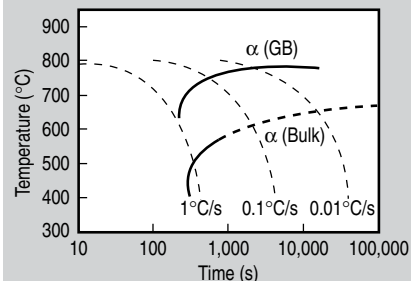


Figure 7. The calculated CCT diagram for Ti-1023.

calculations provide critical information concerning the composition of the γ' and allow the calculation of the γ/γ' interfacial energy (σ) in the relevant kinetic equation. Figure 8 compares experimentally observed and calculated growth rates of γ' in numerous commercial alloys and binary Ni-Al alloys over wide ranges of temperature. The agreement is quite startling for commercial alloys, with the only significant deviation between calculation and experiment being for binary nickel alloys at low temperatures. This can be directly correlated to their larger lattice γ/γ' misfit (δ) in comparison to those found in commercial alloys and means that as long as δ remains $<0.4\%$, which is the more usual case for nickel-based superalloys, the calculations will provide good quality predictions.³⁸

MECHANICAL PROPERTIES

Solid-Solution-Strengthened Alloys

The yield or proof stress of single-phase materials has been calculated using the standard Hall-Petch equation.⁴² Two types of databases for solid-solution hardening have been created, one for flow stress and the other for Hall-Petch coefficients. Both are similar in format to those used for physical properties. There is agreement between calculated and experimentally observed proof stress of a wide range of solution-strengthened alloys. It is further possible to calculate the ultimate tensile stress (UTS) from the calculated value of proof stress using standard relationships

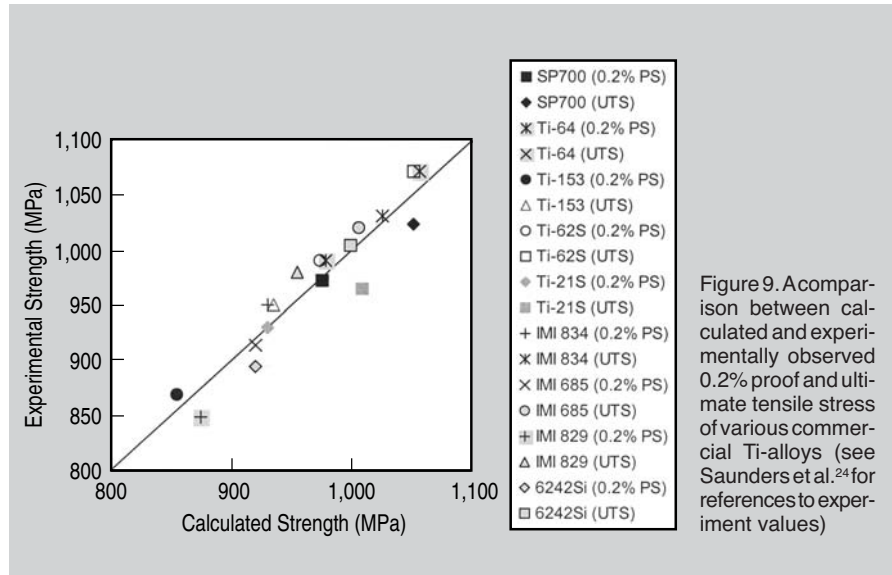


Figure 9. A comparison between calculated and experimentally observed 0.2% proof and ultimate tensile stress of various commercial Ti-alloys (see Saunders et al.²⁴ for references to experiment values)

linking proof and UTS.^{2,43} Figure 9 shows the agreement found for proof stress and UTS for a variety of commercial titanium alloys.²⁴

γ' and γ'' Hardened Ni-Based Superalloys

In nickel-based superalloys strengthened by ordered γ' precipitates, dislocations typically travel in pairs so that their passage through a γ' particle restores perfect order on the $\{111\}$ slip plane. When the particle is small, the yield (or proof) stress is determined by the stress that is necessary to move weakly coupled dislocation pairs. In this case, the first dislocation bows out and the second dislocation remains straight. Following Brown and Ham,⁴⁴ the yield stress can be calculated as described in Reference 2.

When the particles become large, the coupling of the dislocations can

become particularly strong because both dislocations may reside in the same particle. Hüther and Reppich⁴⁵ have analyzed this situation for spherical ordered precipitates and have derived a formula in which the yield stress (CRSS in their original paper) decreases with increasing particle size. Most of the input into the relevant equations can be calculated through an equilibrium thermodynamic calculation and by using the assessed databases for modulus and solid-solution strengthening. However, the most critical factor was found to be the APB energy, which was obtained from a thermodynamic calculation route described previously.^{30,46}

Figure 10 shows the typical behavior associated with hardening by γ' particles as a function of particle diameter; experimental data here are from Mitchell.⁴⁷ There is, initially, a steep rise in strength where the deformation mechanism is dominated by small particle effects. A peak is reached, after which the effect of dislocation coupling becomes more important and the strength then decreases with increasing size of γ' particles. Calculations have also been made for a number of commercial superalloys² where specific information on γ' size is available and compared with experiment (see Reference 2). The agreement is very good. Where size distributions are bi-modal or higher, the amount of γ' at the final heat treatment temperature has been used for the calculation and the total strength obtained by a simple summation of the strengthening effect of the various size distributions.^{48,49}

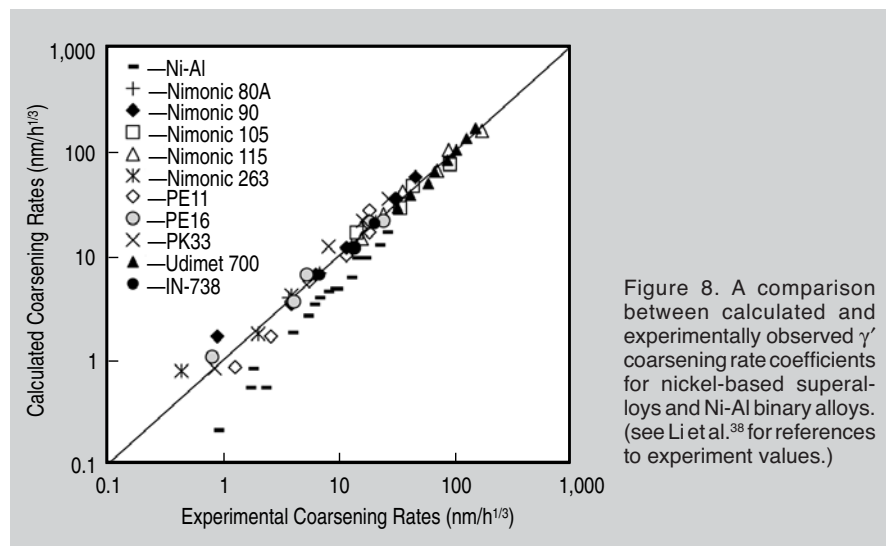


Figure 8. A comparison between calculated and experimentally observed γ' coarsening rate coefficients for nickel-based superalloys and Ni-Al binary alloys. (see Li et al.³⁸ for references to experiment values.)

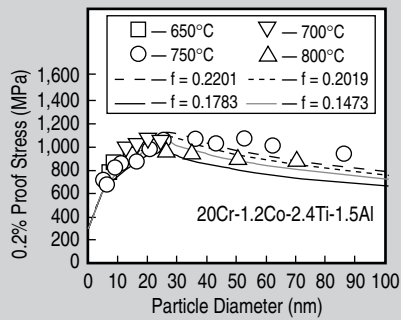


Figure 10. A comparison between calculated and experimental⁴⁷ 0.2% proof stress as a function of γ' size and volume. γ' amounts are those calculated at the respective aging temperature.

γ'' is an ordered superlattice, similarly to γ' , and based on the face-centered cubic gamma structure. A similar mechanism of dislocation strengthening occurs. However, the crystal structure is tetragonal and large coherency strains exist on the major axis. This gives rise to an additional strain-hardening contribution that must be taken into account, and this has been successfully achieved.

High-Temperature Mechanical Properties

For many purposes, knowledge of room-temperature mechanical properties is adequate. However, modeling of properties at high temperature is becoming increasingly important both for component behavior in service and for process modeling (i.e., forging simulations). To this end, the effect of elevated temperatures on tensile properties as well as the modeling of creep in nickel-based superalloys has been undertaken.

Creep

The present work⁵⁰ uses a formulation for the secondary creep rate⁵¹ that features a back stress function and takes the stacking fault energy (γ_{SFE}) explicitly into account.⁵² This approach was selected as it contains parameters that have an identifiable physical basis and that can be calculated self-consistently.

As rupture strength is an alternative design criterion in many practical cases, the calculation procedure has been extended⁵¹ to include this property by

using the relationship suggested by Davies and Wilshire⁵³ where the time to rupture is inversely proportional to the secondary creep rate. Using this correlation it is now possible to make a calculation for creep rupture properties and validate against data for 1,000 h rupture strength for γ' and/or γ'' hardened disk alloys reported by Sims et al. (Figure 11).⁵⁴

Considering the relatively simple approach used in the present study, there is quite remarkable success. It is, however, well understood that the complete modeling of creep will be more complex. For example, a more detailed treatment of microstructural stability should be included. In this case, the coarsening module within *JMatPro* can be used to provide an estimate of the particle size as a function of time at temperature and hence the resulting degradation of properties estimated. This capability will be integrated within the creep module alongside a better representation of damage accumulation leading to a more explicit formulation for the tertiary stage of creep.

However, even with its present shortcomings, it is clear that the present approach has distinct advantages in that very few empirical parameters are required, the model has an identifiable physical basis, and the calculations are self-consistent. The model will now be extended so as to include a full creep curve and it should also be possible to include the susceptibility to rafting for single crystals as *JMatPro* has both a capability to accurately calculate

γ/γ' lattice misfit and make requisite modulus calculations.

High-Temperature Tensile Properties

It is instructive to indicate the present state of work on the calculation of high-temperature tensile properties using a nickel-based superalloy as an example. In this case, the authors combined the 0.2% proof stress of solid solutions as a function of temperature and strain rate, an increasing strength of γ' with temperature, the creep behavior, and the equilibrium dissolution of γ' above the alloy's final heat treatment of 850°C. Figure 12 shows the calculated yield strength of Nimonic 105 as a function of temperature and at a strain rate of 0.002 min.⁻¹ and compares with experimentally reported results from Betteridge.⁵⁵ This accuracy of result is typical of calculations for other alloys ranging from solid-solution alloys, such as Nimonic 75, to high γ' alloys such as PWA1480. The calculations show the transition between the low-temperature region, which is controlled by conventional yield processes, and the higher-temperature region where deformation proceeds via creep. In the creep-controlled region, the alloy is further weakened by the gradual removal of γ' to the point that, above its γ' solvus of 1,025°C, it becomes fully γ .

CONCLUSIONS

JMatPro emphasizes calculation methods that are based on sound physical principles rather than purely statistical methods. In this way, many of the shortcomings of methods such as

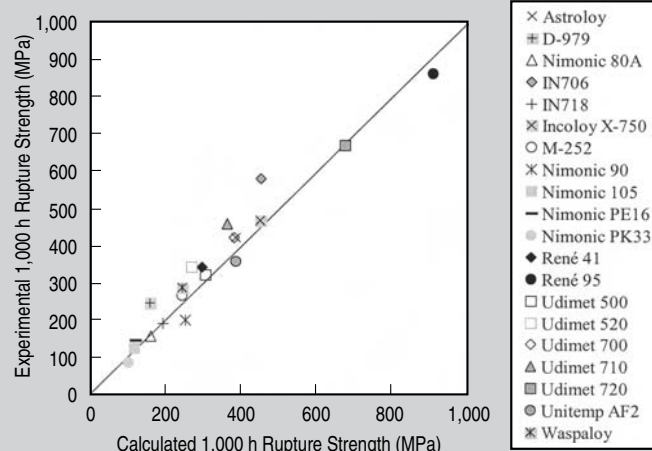


Figure 11. A comparison between calculated and experimentally observed⁵⁴ 1,000 h rupture strength for various nickel-based superalloys.

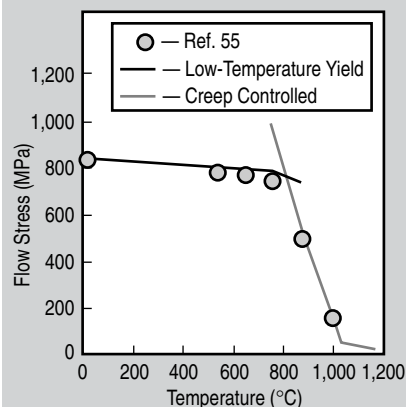


Figure 12. A comparison between calculated and experimentally observed⁵⁶ flow stress as a function of temperature for a Nimonic 105 Ni-based superalloy.

regression analysis are overcome. The inclusion of microstructurally sensitive parameters means that it is possible to make the link with materials models that are currently being developed for prediction of microstructure. This makes it quite feasible to foresee, in the near future, the development of a true virtual capability for design and optimization of thermo-mechanical heat-treatment schedules for many different types of new alloys as well as existing ones. The use of physically based models also means that the true inter-relationship between properties has been developed for complex situations such as in the modeling of creep and precipitation hardening. A key factor in the success of the approach has been the extensive validation of calculated results against experiment.

References

1. N. Saunders and A.P. Miodownik, *CALPHAD—Calculation of Phase Diagrams*, Pergamon Materials Series, vol. 1, ed. R.W. Cahn (Oxford: Elsevier Science, 1998).
2. N. Saunders et al., *Materials Design Approaches and Experiences*, ed. J.-C. Zhao et al. (Warrendale, PA: TMS, 2001), p. 185.
3. H.L. Lukas, J. Weiss, and E.-Th. Henig, *CALPHAD*, 6 (1982), p. 229.
4. U.R. Kattner, W.J. Boettinger, and S.R. Coriell, *Z. Metallkde.*, 87 (1996), p. 522.
5. Z. Fan, P. Tsakiroopoulos, and A.P. Miodownik, *J. Mater. Sci.*, 29 (1994), p. 141.
6. Z. Fan, *Phil. Mag. A*, 73 (1996), p. 1663.
7. A.P. Miodownik, N. Saunders, and J.-P. Schillé, unpublished research.
8. I.B. Fieldhouse and J.I. Lang, *U.S. Air Force Report, WADD-TR-69-904* (1961).
9. H. Leggett et al., *U.S. Air Force Report, AFML-TR-65-147* (1965).
10. B.L. Rhodes et al., *Adv. Cryogenic Engineering*, 8 (1963), p. 278.
11. W.J. Boettinger et al., *Modeling of Casting, Welding and Advanced Solidification Processes VII*, ed. M. Cross et al. (Warrendale, PA: TMS, 1995), p. 649.
12. N. Saunders, *Superalloys 1996*, ed. R. Kissinger et al. (Warrendale, PA: TMS, 1996), p. 115.
13. B.A. Boutwell et al., *Superalloys 718, 625, 706 and Various Derivatives*, ed. E.A. Loria, (Warrendale, PA: TMS, 1996), p. 99.
14. N. Saunders, *Materials Science Forum*, 217-222 (1996), p. 667.
15. N. Saunders, *Light Metals 1997*, ed. R. Huglen (Warrendale, PA: TMS, 1997), p. 911.
16. R.A. Harding and N. Saunders, *Trans. American Foundryman's Society*, 105 (1997), p. 451.
17. N. Saunders, *Solidification Processing 1997*, ed. J. Beech and H. Jones (Sheffield: Univ. Sheffield, 1997), p. 362.
18. N. Saunders, *J. JILM*, 51 (2001), p. 141.
19. N. Saunders et al., *Modeling of Casting, Welding and Advanced Solidification Processes X*, ed. D. Stefanescu et al. (Warrendale, PA: TMS, 2003), p. 669.
20. L. Backerud, E. Krol, and J. Tamminen, *Solidification Characteristics of Aluminium Alloys: Vols. 1 and 2* (Oslo: Tangen Trykk A/S, 1986).
21. N. Saunders et al., *Light Metals 2003*, ed. P. Crepeau (Warrendale, PA: TMS, 2003), p. 999.
22. N. Saunders et al., *Magnesium Technology 2003*, ed. H.I. Kaplan, (Warrendale, PA: TMS, 2003), p. 135.
23. N. Saunders et al., "Modeling of the Thermo-Physical and Physical Properties for Solidification of Ni-based Superalloys" *Proc. Conf. Liquid Metal Processing 2003*, eds. P.D. Lee et al., pp. 253-260.
24. N. Saunders et al., to be published in *Proc. Conf. Ti-2003*.
25. D.A. Porter and K.E. Easterling, *Phase Transformations in Metals and Alloys* (London: Chapman & Hall, 1992).
26. X. Li, A.P. Miodownik, and N. Saunders, *Mater. Sci. Tech.*, 18 (2002), p. 861.
27. J.W. Martin, R.D. Doherty, and B. Cantor, *Stability of Microstructure in Metallic Systems* (Cambridge: Cambridge University Press, 1997).
28. J.O. Nilsson and A. Wilson, *Materials Science and Technology*, 9 (1993), p. 545.
29. C.M.F. Rae et al., *Superalloys 2000*, ed. K.A. Green et al. (Warrendale, PA: TMS, 2000), p. 767.
30. N. Saunders, M. Fahrman, and C.J. Small, *Superalloys 2000*, ed. K.A. Green et al. (Warrendale, PA: TMS, 2000), p. 803.
31. A. Oradei-Basile and J.F. Radavich, *Superalloys 718, 625 and Various Derivatives (1991)*, ed. E.A. Loria (Warrendale, PA: TMS, 1991), p. 325.
32. R.B. Nicholson, *Phase Transformations* (Materials Park, OH: ASM, 1970), p. 269.
33. J.R. Toran and R.R. Biederman, *Titanium Science and Technology*, ed. H. Kimura and O. Izumi (Warrendale, PA: Met. Soc. AIME, 1980), p. 1491.
34. S. Bein and J. Bechet, *Titanium '95*, ed. P. Bleckinsop et al. (London: The Institute of Materials, 1996), p. 2353.
35. J.S. Kirkaldy, *Scand. J. Metall.*, 20 (1991), p. 50.
36. J.S. Kirkaldy, B.A. Thomson, and E.A. Baganis, *Hardenability Concepts with Applications to Steel*, ed. J.S. Kirkaldy and D.V. Doane (Warrendale, PA: AIME, 1978), p. 82.
37. J.S. Kirkaldy and D. Venugopalan, *Phase Transformations in Ferrous Alloys*, ed. A.R. Marder and J.I. Goldstein (Warrendale, PA: AIME, 1984), p. 125.
38. X. Li, N. Saunders, and A.P. Miodownik, *Metall. Mater. Trans. A*, 33A (2002), p. 3367.
39. I.M. Lifshitz and V.V. Slyozov, *J. Phys. Chem. Solids*, 19 (1961), p. 35.
40. C. Wagner, *Z. Elektrochem.*, 65 (1961), p. 581.
41. H.A. Calderon et al., *Acta Metall.*, 42 (1994), p. 991.
42. E.O. Hall, *Yield Point Phenomena in Metals and Alloys* (London: Macmillan, 1970), p. 38.
43. X. Li, A.P. Miodownik, and N. Saunders, *J. Phase Equilibria*, 22 (2001), p. 247.
44. L.M. Brown and R.K. Ham, *Strengthening Mechanisms in Crystals* (London: Applied Science, 1971).
45. W. Hüther and B. Reppich, *Z. Metallkde.*, 69 (1978), p. 628.
46. A.P. Miodownik and N. Saunders, *Applications of Thermodynamics in the Synthesis and Processing of Materials*, ed. P. Nash and B. Sundman (Warrendale, PA: TMS, 1995), p. 91.
47. V.W.I. Mitchell, *Z. Metallkde.*, 7 (1966), p. 586.
48. B. Reppich et al., *Mater. Sci. Eng.*, 83 (1986), p. 45.
49. D.J. Chellman, A.J. Luévano, and A.J. Ardell, *Strength of Metals and Alloys* (London: Freund Publishing House, 1991), p. 537.
50. A.P. Miodownik et al., "Modeling of Creep in Nickel Based Superalloys," to be published in *Proc. Conf. 6th International Charles Parsons Turbine Conference*, eds. A. Strang et al., (London: Maney, 2003), pp. 779-788.
51. X.S. Xie et al., *Scripta Metall.*, 16 (1982), p. 483.
52. C.R. Barrett and O.D. Sherby, *Trans. Met. Soc. AIME*, 233 (1965), p. 1116.
53. P.W. Davies and B. Wilshire, *Structural Processes in Creep*, ed. A.G. Quarrell (London: Iron and Steel Institute, 1961), p. 34.
54. C.T. Sims et al. editors, *Superalloys II* (New York: Wiley & Sons, 1987).
55. W. Betteridge and J. Heslop, *The NIMONIC Alloys and Other Ni-Based High Temperature Alloys: 2nd ed.*, (London: Edward Arnold, 1974).
56. F.B. Pickering, *Physical Metallurgy and the Design of Steels* (London: Applied Science Publishers, 1978).

N. Saunders is a technical director with Thermotech Ltd. in Guildford, U.K. Z. Guo and X. Li are senior materials scientists, A.P. Miodownik is a senior consulting scientist, and J.-Ph. Schillé is a technical director with Sente Software Ltd. in Guildford, U.K.

For more information, contact N. Saunders, Thermotech Ltd., Surrey Technology Centre, The Surrey Research Park, Guildford GU2 7YG, U.K.; +44-1483-685470; fax +44-1483-685472; e-mail nigel.saunders@thermotech.co.uk.

What's new at TMS On-Line?

The TMS web site brings you continual updates of the latest society information. What's new this month? Visit the TMS web site to find:

- Plan your schedule for the 2004 TMS Annual Meeting through the TMS Personal Conference Scheduler, at <http://pcs.tms.org>.
- Continue your education with the society's first on-line short course, Metal-Matrix Composites, at www.tms.org/Education/ceo-mmc.html.
- Read the December issue of JOM-e on-line only at www.tms.org/jom.html.

Visit the site regularly and click on "What's New" to find out the most up-to-date information on meetings, publications, membership activities, and more.

www.tms.org